

GRANT/GOLDWARD

31p.

Data Processing and Case Study Analysis  
of Thunderstorm Studies

IN -  
34295

Final Report

Michael R. Poellot  
Principal Investigator

June 1, 1985 to November 30, 1986

Department of Atmospheric Sciences  
University of North Dakota  
Box 8216 University Station  
Grand Forks, ND 58201-8216

NASA Grant No. NAG 5-541

(NASA-CR-179890) DATA PROCESSING AND CASE  
STUDY ANALYSIS OF THUNDERSTORM STUDIES  
Final Report (North Dakota Univ.) 31 p

N87-12083

CSCL 04B

G3/47

Unclas  
44788

## I. Overview and Objectives

During May, 1984, the University of North Dakota (UND) operated an instrumented research aircraft in support of NASA/GSFC ER-2 thunderstorm studies. The objective of the UND operations was to provide in situ measurements of cloud microphysical parameters during ER-2 cloud overflight missions. These data were initially provided to NASA scientists in an archive format. Under Grant No. NAG 5-541 UND has provided further processing of the data and a case study analysis of the data collected on one of the missions.

UND became involved in this measurement program at the request of NASA scientists in order to support certain on-going research efforts at the GSFC. One such effort is the development and interpretation of lidar cloud top observations by J. Spinhirne and others at Goddard (Spinhirne, et al., 1983). The backscatter signal intensities and linear depolarization ratios of the lidar signals are dependent on the physical composition of the target clouds and can be used to infer information concerning the dynamics and development of cloud systems. However, a dearth of supporting in situ cloud measurements has made it necessary to assume certain cloud microphysical properties when interpreting the lidar data. The data gathered during these field studies will enable a direct comparison of lidar observations and cloud properties to be made, thereby reducing some of the uncertainty of these interpretations.

Other Goddard scientists have examined cloud top characteristics associated with severe storms (Heymsfield, et al., 1983). Of particular interest has been the "V" pattern observed in severe thunderstorm anvils. There have been a number of explanations proposed for this phenomenon, but again, in situ measurements of cloud microphysical and dynamical properties are needed to determine which mechanism(s) are at work.

The mission profiles for the field studies were therefore designed to examine in detail the cloud top structure of a number of cloud types, including cirrus, altostratus/altocumulus, and severe thunderstorms. Although no severe storms were sampled during the period of UND operations, thunderstorms with overshooting tops were studied along with the other cloud objectives. These flight operations were closely coordinated within the given constraints of air traffic control and instrumentation. Visual contact between the aircraft crews on several occasions verified the proximity of the observations in time and space.

The second mission of the period (May 19) was particularly interesting as it was flown through portions of a multicell thunderstorm with overshooting tops. Frequent penetrations of these turrets along with several traverses of the downwind anvil were made with the UND plane while ER-2 overflights were conducted. Also, by good fortune, this system evolved within the coverage area of the NSSL Doppler radars, offering another view of its development. The multiplicity of special observations along with standard atmospheric measurements offered a rare

opportunity to examine the upper-level structure of a thunderstorm and its interactions with its environment.

The objectives of the work under this grant were twofold:

1. to further process the data collected by the UND Citation aircraft through interpretive software; and
2. to perform a case study analysis of the anvil top structure of the May 19, 1984 thunderstorm.

The case study was a collaborative effort between UND and GSFC scientists, primarily Dr. Gerald Heymsfield. Principal Investigator Michael Poellot and Dr. Heymsfield were on board the Citation on 19 May for this mission.

## II. Data Processing and Analysis

The work done under this contract was conducted in two phases. Phase I entailed the data processing and transfer of the output products to NASA. Phase II included the case study analysis.

### Phase I - Data Processing

During the study period, three coordinated missions were flown with the UND Citation for a total of 13.5 flight hours. Sampling parameters for the in situ aircraft included three dimensional winds, cloud microphysics and the state parameters. Time lapse and hand-held photographs are also available.

The primary data collected during the field studies were provided on magnetic tape to NASA under an earlier grant. Except for the PMS probe information, these data were initially processed from the raw digital and binary numbers into real and integer values. The data are archived in this form at UND.

Additional processing was required for conversion to engineering units and examination of the data. Under the first phase of the grant hardcopy output products were provided to NASA. Appendix A includes a mission summary for each of the three flights and a list of products provided for each mission. Also included in the Appendix is a brief explanation of output parameters and graphics.

The bulk of the data, other than PMS and wind information, was converted using standard equations, as found in Veal, et al., (1977). These data (e.g., state parameters, INS tracking, etc.) were presented in the form of listings and time series plots. Two-dimensional flight tracks were also produced to assist with data interpretation.

The Citation carries a set of PMS probes which cover the cloud particle size distribution from cloud droplets (FSSP) to large precipitation particles (1DP). A PMS 2DC probe provides images of particles greater than 35 um. These are standard instruments

except the 2DC has been adjusted for a higher than standard airspeed with an effective 35  $\mu\text{m}$  diode spacing instead of the usual 25  $\mu\text{m}$ .

These instruments are capable of resolving a single particle; however, their accuracy depends on the particular application. The optical array probes (2DC and LDP) in general do not suffer from the activity and spectral shifting problems experienced by light scattering instruments such as the FSSP. They do suffer from artifacts caused by water in the beam ("streakers") and particles shattering on the probe arms. These problems interfere with counting low ice concentrations in regions of high liquid water (Baumgardner and Dye, 1983). UND employs the methods of Cooper (1978) to omit artifacts from the processed 2D data. This method rejects particles which are too long in the direction of flight (streaker images), and particles with gaps or too short an interval between particles (splash images). Similar corrections are not available for the LDP; however, examination of the artifact frequency in the 2DC is helpful in discerning when artifacts are likely to present in the LDP.

Although the software corrections greatly improve the utility of the 2D data, experience has shown that it is still necessary to examine the images manually to ascertain that the software corrections are producing the desired results. The same software is also capable of discerning ice from water, which is quite useful in computing parameters which depend on the size and type of particle, such as rainfall rate.

The PMS data were processed through several different routines to apply the above corrections, compute statistical quantities and display the derived information. Computed parameters are listed in Table 1. These values have been listed and plotted as time series. The particle size spectra were also output along with the 2D particle images.

The three dimensional winds were computed utilizing the method described by Lenschow (1972), using outputs from the flow angle probe mounted on the nose boom of the aircraft and the INS mounted near the center of gravity. The wind vector equation is

$$\mathbf{V}_{w/e} = \mathbf{V}_{w/p} + \mathbf{V}_{p/e} + \boldsymbol{\Omega} \times \mathbf{R}$$

The first term on the right is the wind velocity relative to the plane. It is the airspeed resolved through the attack and sideslip angles into the aircraft body axes. This vector is

Table 1. UND Citation Computed Cloud Microphysical Parameters

<u>Probe</u>	<u>Parameters</u>
FSSP	Raw counts, particle concentrations Mean volume diameter and standard deviation Cloud liquid water content
1DP	Raw counts, particle concentrations Mean volume diameter and standard deviation Water equivalent rain rate and radar reflectivity Ice equivalent rain rate and radar reflectivity
2DC	Particle concentrations Total accepted and rejected particles Ice water concentration Mean volume diameter and standard deviation Water equivalent rain rate and radar reflectivity Ice equivalent rain rate and radar reflectivity
Ice Detect	Cloud liquid water content
J-W	Liquid water concentration

then transformed into earth axes through an Eulerian transformation. The second term is the velocity of the plane with respect to the earth and is obtained from the INS. The North and East components are found from the ground speed and track angle. The vertical velocity is obtained by integrating the vertical accelerometer output and is damped by a second order lag. The final term accounts for the spatial separation of the flow angle probe and INS and the angular accelerations of the aircraft.

Bias errors in the horizontal winds (u,v components) of the type cited in Grossman (1977) have been removed from the data using reverse heading data. Several portions of each flight were examined and correction factors determined and applied as necessary in the form of an adjustment to the computed true airspeed. Biases in the vertical winds were removed by applying calibration factors which yield a net zero value when averaged over a long leg out of cloud in smooth air. Nominal accuracies for the horizontal wind speed and direction and the vertical wind component are estimated to be  $\pm 2 \text{ msec}^{-1}$ ,  $5^\circ$  and  $\pm 1 \text{ msec}^{-1}$ , respectively.

Wind data were both listed and plotted as time series of direction, horizontal velocity and vertical velocity. A two-dimensional display of the horizontal winds along the flight track was also provided.

## Phase II - Case Study Analysis of May 19, 1984 Data

The coordinated aircraft mission of May 19 was conducted in the vicinity of a cumulonimbus complex over Oklahoma. Although the initial study clouds were some distance to the east, the aircraft were drawn to the Norman, OK, area by visual observations of cumuliform thunderstorm tops. The aircraft arrived on station during the mature phase of the storm. The system appeared to have a multicellular structure and was long-lived, allowing aircraft measurements for almost two hours. Based on aircraft and radar observations the storm was not classified as severe. However, it did send up towers that rose 0.5 to 1.0 km above the mean top of the cirrus which was around 12 km. The anvil cloud was relatively narrow and extended northward roughly 50 km downwind.

The objectives of the May 19 case study analysis were:

- to determine the interactions between the thunderstorm overshooting tops and their environment, and
- to examine the persistence of storm-induced perturbations in the anvil structure.

This study examined the microphysical, dynamic and thermodynamic characteristics of the overshooting tops and the downwind cirrus anvil top. This included spatial and temporal distributions of cloud particle types and concentrations, horizontal and vertical winds in the cloud and its vicinity, and profiles of thermodynamic parameters. The results of the study were presented at the 23rd Radar Conference and Conference on Cloud Physics at Snowmass in a paper entitled "Structure of an Oklahoma Storm Top from In Situ Measurements" (Poellot and Heymsfield, 1986). The text from the conference Preprints is included as Appendix B.

er-861028  
tsfinal.dta/1103

## REFERENCES

- Baumgardner, D. and J. Dye, 1983: The 1982 Cloud Particle Measurement Symposium. Bull. Amer. Meteor. Soc., 64, 336-370.
- Cooper, W.A., 1978: Cloud physics investigations by the University of Wyoming in HIPLEX 1977. Final Report, University of Wyoming, Laramie, WY., 320 pp.
- Grossman, R.L., 1977: A procedure for the correction of biases in winds measured from aircraft. J. Appl. Meteor., 16, 654-658.
- Heymsfield, G.M., R.H. Blackmer, Jr. and S. Schotz, 1983: Upper-level structure of Oklahoma tornadic storms on 2 May, 1979. I: Radar and satellite observations. J. Atmos. Sci., 40, 1740-1755.
- Heymsfield, G.M., G. Szejwach, S. Schotz and R.H. Blackmer, Jr., 1983: Upper-level structure of Oklahoma Tornadic Storms on 2 May 1979. II: Proposed explanation of "V" pattern and internal warm region in infrared observations. J. Atmos. Sci., 40, 1756-1767.
- Lenschow, D.H., 1972: The measurement of air velocity and temperature using the NCAR Buffalo aircraft measuring system. NCAR Tech. Note EDD - 74.
- Poellot, M.R., and G.M. Heymsfield, 1986: Structure of an Oklahoma Storm Top from In Situ Measurements. Preprints, 23rd Conference on Radar Meteorology and Conference on Cloud Physics, (Snowmass). J61-64.
- Spinhirne, J.D., M.Z. Hansen and J. Simpson, 1983: The structure and phase of cloud tops as observed by polarization lidar. J. Climate and Appl. Meteor., 22, 1319-1331.
- Veal, D.L., W.A. Cooper, G. Vali and J.D. Marwitz, 1977: Some aspects of aircraft instrumentation for storm research. Meteorol. Monographs, 16, 237-255.

**Appendix A**

**Mission Summaries  
and  
Data Products**



May 18, 1984  
UND Citation Mission

GMT Time	Altitude	Lat	Lon	Event	
20:11:15	39,000'	39-47	94-40	Start Line 1	Thin Ci patch
20:26:00		40-33	93-28	End Line 1	No 2-D images
20:31:00	39,000'	40-34	93-27	Start Line 2	No 2-D images
20:49:00		39-54	94-33	End Line 2	
20:53:00	39,000'	39-56	94-30	Start Line 3	Not processed
20:58:30		40-13	94-02	End Line 3	does not overlap ER-2
21:14:00	33,000'	40-16	94-14	Start Line 4	
21:29:30		40-16	95-47	End Line 4	
21:39:30	18,500'	40-35	96-32	Start Line 5	As, Ac deck
21:50:15		40-45	97-09	End Line 5	
21:53:00	18,300'	40-45	97-10	Start Line 6	
22:02:00		40-35	96-36	End Line 6	
22:05:30	18,000'	40-36	96-36	Start Line 7	
22:14:30	18,200'	40-45	97-09	End Line 7	
22:18:45	12,500'	40-44	97-07	Start Line 8	
22:26:45	7,300'	40-36	96-37	End Line 8	

Processed UND Citation Data for 5/18/84

Data Times

GMT - 2 hours (clock was incorrectly set)

Data Segments

from Citation flight legs which overlapped with ER-2 flight lines.

Outputs

A brief explanation of output parameters and graphics is attached.

- LIST - one second data listing
- PLOTS - time plots of parameters
- PMSCOM - listing of derived parameters and 2-D images
- PMSPLIT - time plots of derived parameters
- PMSIZE - particle size spectra
- TRACK - plots of horizontal winds along flight tracks
- ASQUI - ASCII tape of one second data

## LIST

A brief description of the variable names follows.

ALT\* = INS altitude  
PRALT = Pressure altitude  
STATP = Static pressure  
IAS = Indicated air speed  
TAS = True air speed  
GRND = Ground speed  
NOSER = Pitotstatic pressure from the nose transducer  
NOSES = Pitotstatic pressure from the standby transducer  
WING = Pitotstatic pressure from the wing transducer  
ATEMP = Air temperature (Rosemount sensor)  
TTEMP = Rosemount (total) temperature  
REVRS = Air temperature (Reverse flow sensor) (inop)  
DWPNT = Dew point temperature  
VACCN = Vertical acceleration  
VACCG = (vertical acceleration) \* X, X < 1.0  
ICE = Ice rate meter  
JW = Johnson-Williams liquid water content  
ATTCK = Angle of attack  
SDSLP = Angle of sideslip

TRUE = True heading  
TRACK = Track angle  
INS = Internal INS reference  
DRIFT = Drift angle  
MAG = Magnetic heading  
VOR = VORTAC radial  
DME = TACAN distance  
PIT C = Pitch angle (+/- 180.0)  
PIT F = Pitch angle (+/- 22.5)  
ROL C = Roll angle (+/- 180.0)  
ROL F = Roll angle (+/- 22.5)  
WINDD = Calculated wind direction  
WINDS = Calculated wind speed

BINFT = Internal INS parameter  
AC xx = Spares  
FL = INI flag  
ST = INS status  
WINDD = INS wind direction  
WINDS = INS wind speed  
SEC24 = Seconds from midnight  
SEC1 = Seconds from midnight  
INTSEC = Interval seconds remaining

## PLOTS

Parameters chosen:

<u>Segment</u>	<u>Parameters</u>
Entire flight overview	Pressure altitude, static pressure, temperature
All flight segments	Temperature, dew point, static pressure, wind direction and speed, Theta E
Lower level segments	JW liquid water, icing rate meter derived supercooled water conc.

May 19, 1984  
UND Citation Mission

GMT Time	Altitude	Lat	Lon	Event	
20:54:00	40,800'	34-44	95-45	Start Line 1	
21:01:00		34-15	95-52	End Line 1	
21:22:30	40,800'	35-13	97-38	Start Line 2	Tower penetration
21:28:00		35-45	97-35	End Line 2	Anvil run, S-N
21:36:30	40,800'	35-49	97-34	Start Line 3	Anvil run, N-S
21:46:30		35-42	97-30	End Line 3	Tower penetration
21:50:00	39,200'	35-13	97-32	Start Line 4	Tower penetration
21:51:15		35-09	97-32	End Line 4	N-S
21:58:30	41,000'	35-21	97-31	Start Line 5	Over top of
22:00:15		35-14	97-32	End Line 5	turret, N-S
22:04:30	40,800'	35-12	97-30	Start Line 6	Tower penetration
22:06:30	39,000'	35-23	97-29	End Line 6	S-N
22:11:30	39,200'	35-22	97-29	Start Line 7	Tower penetration
22:14:15		35-11	97-32	End Line 7	N-S
22:17:00	40,000'	35-14	97-31	Start Line 8	Penetration, S-N,
22:17:45		35-18	97-29	End Line 8	in & out of tops
22:20:00	40,000'	35-20	97-28	Start Line 9	Penetration, W-E,
22:20:45	39,800'	35-20	97-24	End Line 9	downwind side
22:24:00	40,000'	35-33	97-22	Start Line 10	Anvil crossing E-W
22:25:00		35-34	97-27	End Line 10	decaying push
22:31:45	39,000'	35-41	97-22	Start Line 11	Anvil run, N-S
22:36:30		35-25	97-27	End Line 11	
22:39:45	39,000'	35-21	97-25	Start Line 12	N-S anvil,
22:46:15	40,300'	34-59	97-23	End Line 12	jog in the line
22:48:00	41,000'	35-04	97-17	Start Line 13	Tower penetration
22:54:45	39,000'	35-33	97-14	End Line 13	S-N, anvil
23:04:30	37,000'	35-34	97-09	Start Line 14	Anvil N-S
23:14:15		35-03	97-11	End Line 14	

## Processed UND Citation Data for 5/19/84

### Data Times

All time are GMT

### Data Segments

from Citation flight legs which overlapped with ER-2 flight lines and from penetrations of overshooting tops.

### Outputs

A brief explanation of output parameters and graphics is attached.

- LIST - one second data listing
- PLOTS - time plots of parameters
- PMSCOM - listing of derived parameters and 2-D images
- PMSPLIT - time plots of derived parameters
- PMSIZE - particle size spectra
- TRACK - plots of horizontal winds along flight tracks
- ASQUI - ASCII tape of one second data
- WINDS - time plots of vertical winds and listings  
of calculated three-dimensional winds

## PLOTS

Parameters chosen:

<u>Segment</u>	<u>Parameters</u>
Entire flight overview	Pressure altitude, static pressure, temperature
All flight segments	Wind direction and speed, Theta E

May 22, 1984  
UND Citation Mission

GMT Time	Altitude	Lat	Lon	Event	
21:44:45	41,000'	38-13	91-27	Start Line 1	SW-NE
21:59:15	39,000'	38-48	90-03	End Line 1	
22:08:15	39,000'	38-54	90-21	Start Line 2	Not processed - no ER-2 overlap
22:11:00		38-50	90-34	End Line 2	
22:11:00	39,000'	38-50	90-34	Start Line 3	Cross anvil Right jog
22:18:30		38-20	90-19	End Line 3	
22:21:30	38,600'	38-23	90-09	Start Line 4	Not processed - no ER-2 overlap
22:30:00	38,800'	38-57	90-23	End Line 4	
22:42:00	39,000'	39-06	90-09	Start Line 5	Not processed - no ER-2 overlap
22:45:15		38-54	90-00	End Line 5	
22:45:15	39,000'	38-54	90-00	Start Line 6	Not processed - TAS invalid
22:48:15		38-46	90-06	End Line 6	
22:59:00	39,000'	38-25	90-04	Start Line 7	Not processed - TAS invalid
23:09:00	37,000'	39-10	90-43	End Line 7	
23:50:00	22,000'	38-34	91-51	Start Line 8	AltoCu, E-W
00:12:15	19,800'	38-29	93-02	End line 8	
00:15:00	19,400'	38-30	93-02	Start Line 9	W-E
00:27:15		38-34	91-56	End Line 9	
00:31:00	18,400	38-34	91-52	Start Line 10	E-W
00:35:30	13,400	38-33	92-07	End Line 10	



## Processed UND Citation Data for 5/22/84

### Data Times

All time are GMT

### Data Segments

from Citation flight legs which overlapped with ER-2 flight lines. Data were invalid for several lines when derived true airspeeds (TAS) were invalid.

### Outputs

A brief explanation of output parameters and graphics is attached.

- LIST - one second data listing
- PLOTS - time plots of parameters
- PMSCOM - listing of derived parameters and 2-D images
- PMSPLIT - time plots of derived parameters
- PMSIZE - particle size spectra
- TRACK - plots of horizontal winds along flight tracks
- ASQUI - ASCII tape of one second data

## PLOTS

Parameters chosen:

<u>Segment</u>	<u>Parameters</u>
Entire flight overview	Pressure altitude, static pressure, temperature, dew point temperature
All flight segments	Temperature, dew point, static pressure, equivalent potential temperature, wind direction and speed
Lower level segments	JW liquid water

## LIST

A brief description of the variable names follows.

ALT\* = INS altitude  
PRALT = Pressure altitude  
STATP = Static pressure  
IAS = Indicated air speed  
TAS = True air speed  
GRND = Ground speed  
NOSER = Pitotstatic pressure from the nose transducer  
NOSES = Pitotstatic pressure from the standby transducer  
WING = Pitotstatic pressure from the wing transducer  
ATEMP = Air temperature (Rosemount sensor)  
TTEMP = Rosemount (total) temperature  
REVRS = Air temperature (Reverse flow sensor) (inop)  
DWPNT = Dew point temperature  
VACCN = Vertical acceleration  
VACCG = (vertical acceleration) \* X, X < 1.0  
ICE = Ice rate meter  
JW = Johnson-Williams liquid water content  
ATTCK = Angle of attack  
SDSLP = Angle of sideslip

TRUE = True heading  
TRACK = Track angle  
INS = Internal INS reference  
DRIFT = Drift angle  
MAG = Magnetic heading  
VOR = VORTAC radial  
DME = TACAN distance  
PIT C = Pitch angle (+/- 180.0)  
PIT F = Pitch angle (+/- 22.5)  
ROL C = Roll angle (+/- 180.0)  
ROL F = Roll angle (+/- 22.5)  
WINDD = Calculated wind direction  
WINDS = Calculated wind speed

BINDFT = Internal INS parameter  
AC xx = Spares  
FL = INI flag  
ST = INS status  
WINDD = INS wind direction  
WINDS = INS wind speed  
SEC24 = Seconds from midnight  
SEC1 = Seconds from midnight  
INTSEC = Interval seconds remaining

## PMSCOM

Includes printout of every 5th 2-D image and processed  
PMS probe data. 2-D processing based on Cooper scheme.

CHNL	- FSSP size range (#1 = 2-32 microns)
FSSPCONC	- number concentration of FSSP particles (/cm <sup>3</sup> )
1DCONC	- number concentration of 1-D particles (/liter)
VMEANFSSP	- mean volume diameter of FSSP particles (microns)
VMEAN1D	- mean volume diameter of 1-D particles (microns)
VSIGMA1D	- standard deviation of 1-D mean volume diameter
VSIGMAF	- standard deviation of FSSP mean volume diameter
RRG	- equivalent rain rate, assuming graupel density of 0.5 (mm/hour). uses 1-D particle information.
RRW	- equivalent rain rate (mm/hour). uses 1-D particles.
DBZW	- equivalent reflectivity of 1-D particles if water.
DBZG	- equivalent reflectivity of 1-D particles if ice, density 0.5.
LWC	- liquid water content, using FSSP data (g/m <sup>3</sup> )
2DCONC	- number concentration of 2-D particles
VOLCONC	- concentration of 2-D particles, assuming a density of 1. (g/m <sup>3</sup> )
NSTREAKERS	- number of rejected 2-D particles
NICE	- number of accepted 2-D particles
TAS2D	- true airspeed of aircraft (m/s)

## PMSPLOT

The following derived parameters are plotted against time:

N1D        - number concentration of 1-D probe sized particles  
              (#/1)  
VMEAN1D   - volume mean diameter of 1-D particles (microns).  
              not plotted if particle numbers are very small.  
VSIGMA1D   - standard deviation of the 1-D volume mean diameter.  
N2D        - number concentration of 2-D particles (#/1)  
VTOT2D     - volume of 2-D particles per cubic meter assuming  
              sphericity (cm3)  
VMEAN2D   - volume mean diameter of 2-D particles (microns)  
VSIGMA2D   - standard deviation of the 2-D volume mean diameter

PMSIZE

These are plots of average particle spectra over selected time intervals. The abscissa on all plots are channel or size range midpoints (microns).

N(I)/DLOGD - number concentration/cm<sup>3</sup> per delta  
log(size range). (e.g., LOG(4) - LOG(2))

V(I)/DLOGD - volume (in cubic microns) per delta  
log(size range).

TRACK

Plots of winds (in knots) along the flight tracks, at  
one minute intervals.

## WINDS

These are plots of the calculated vertical wind component and the vertical aircraft velocity, along with a listing of the following parameters at one second intervals:

VERTW - vertical component of the wind (m/s)  
HWIND - horizontal wind speed (knots)  
WDIR - horizontal wind direction (degrees)  
TAS - aircraft true airspeed (knots)  
ALT - INS-derived aircraft altitude (feet)  
PRALT - aircraft pressure altitude (feet)  
VACC - vertical aircraft acceleration (m/s/s)  
VVEL - aircraft vertical velocity (m/s)  
ALFA - angle of attack (degrees)  
BETA - angle of sideslip (degrees)



## Description of the ASQUI program

The ASQUI program creates a file of once a second data records in ASCII format. The records may be written to tape or to a disc file for later transfer to tape. Each disc file data record is 512 bytes long. The first six records in each file contain the date of the data and other descriptive information detailing the contents of the data records. The FORMAT used in writing the data is 51F10.3.

The contents of the data records are:

1. Time	(Seconds from Midnight)
2. Altitude	(Meters)
3. Pressure Altitude	(Meters)
4. Static Pressure	(mb)
5. Indicated Air Speed	(Meters/Sec)
6. True Air Speed	(Meters/Sec)
7. Ground Speed	(Meters/Sec)
8. Pitotstatic Pressure, Nose	(mb)
9. Pitotstatic Pressure, Wing	(mb)
10. Rosemount Temperature	(deg-K)
11. Reverse Flow Temperature	(deg-K)
12. Air Temperature, Rosemount	(deg-K)
13. Air Temperature, Reverse Flow	(deg-K)
14. Dew Point	(deg-K)
15. Ice Detector	(Volts)
16. J & W Liquid Water	(100*Volts/TAS)
17. Vortac	(Deg)
18. DME	(Kilometers)
19. Vertical Acceleration	(Meters/Sec**2)
20. Attack Angle	(mb)
21. Side Slip Angle	(mb)
22. Attack Angle	(Deg)
23. Side Slip Angle	(Deg)
24. Vertical Acceleration Gained	(Volts)
25. Vapor Pressure	(mb)
26. Mixing Ratio	(Per Cent)
27. Potential Temperature	(deg-K)
28. Equivalent Potential Temperature	(deg-K)
29. Ice Detector Heater Flag	(Volts)
30. Track Angle	(Deg)
31. Drift Angle	(Deg)
32. True Heading	(Deg)
33. Magnetic Heading	(Deg)
34. Pitch Angle	(Deg)
35. Roll Angle	(Deg)
36. INS Wind Direction	(Deg)
37. INS Wind Velocity	(Meters/Sec)

38. Vertical Velocity	(Meters/Sec)
39. Vertical Wind	(Meters/Sec)
40. Calculated Wind Velocity	(Meters/Sec)
41. Calculated Wind Direction	(Deg)
42. Latitude	(Deg)
43. Longitude	(Deg)
44. Analog Channel 23	(Volts)
45. Analog Channel 24	(Volts)
46. Analog Channel 7	(Volts)
47. Analog Channel 8	(Volts)
48. INS Time	
49. INI Flag	
50. INS Status	
51. Mach Number	

Appendix B

"Structure of an Oklahoma Storm Top  
From In Situ Measurements"

## STRUCTURE OF AN OKLAHOMA STORM TOP FROM IN SITU MEASUREMENTS

Michael R. Poellot  
Department of Atmospheric Sciences  
University of North Dakota  
Grand Forks, North Dakota

Gerald M. Heymsfield  
Laboratory for Atmospheres  
NASA/Goddard Space Flight Center  
Greenbelt, Maryland

### 1. INTRODUCTION

During May, 1984, the University of North Dakota operated an instrumented research aircraft in support of NASA/Goddard ER-2 aircraft thunderstorm studies. The objective of the UND operation was to provide in situ measurements of cloud microphysical parameters during ER-2 cloud overflight missions. The coordinated aircraft mission of May 19 was conducted in the vicinity of a cumulonimbus complex southwest of Norman, Oklahoma. This storm, of moderate intensity, sent up towers which rose 1.0 km above the mean top of the cirrus anvil and it was within the coverage of the NSSL Doppler radars. This paper focuses on the measurements obtained by the UND Citation II aircraft. A detailed analysis of ER-2 and ground-based radar observations is presented by Heymsfield *et al.*, elsewhere in these proceedings.

The nature of overshooting thunderstorm tops and their interaction with their environment is not yet well understood. It is difficult to obtain in situ observations, since these turrets often reach well into the lower stratosphere. Not only is this higher than the service ceiling of most research aircraft, but the severe nature of these systems produces an unfriendly flight environment. Much of our present knowledge is limited to the results of modeling and remote sensing studies.

Characteristic dimensions and growth rates of overshooting domes have been measured remotely for several severe storms by Shenk (1974), Roach (1967) and Adler, *et al.*, (1983). Observed differences between dome heights and the tops of surrounding anvil cloud ranged from a few hundred meters to several kilometers. The depth of penetration into the stratosphere as related to updraft velocities has been modeled by Saunders (1962) and Adler, *et al.*, (1983). Newton (1965) hypothesized that the air in these towers mixes with stratospheric air and returns to lower levels to become part of the anvil plume in the upper troposphere. Roach (1967) and Danielsen (1982), however, favor a trajectory that requires the air to remain largely in the lower stratosphere because the dilution significantly reduces the negative buoyancy of the parcels. Heymsfield, *et al.*, (1983) have postulated that the air flows over these overshooting tops with descending flow on the downwind side.

### 2. GENERAL STORM STRUCTURE AND MEASUREMENTS

The storm of interest developed southwest of Norman and was first scanned by the Cimarron radar at 2100 GMT when it was 30 km west-southwest. Two main cells and a number of smaller reflectivity cores tracked to the east at approximately  $7 \text{ ms}^{-1}$  during the study period. The storm existed in a moderately sheared environment, as illustrated in Fig. 1. Winds from the surface to 550 mb were from the west at  $3 \text{ ms}^{-1}$  increasing with height to  $10 \text{ ms}^{-1}$ . Above this level they backed and strengthened to approximately  $210$  at  $25 \text{ ms}^{-1}$  in the vicinity of the tropopause. The storm itself was strongly sheared, tilting at a  $45^\circ$  angle downwind between 5 km and cloud top (Fig. 2). The overshooting towers at a height of 12 km were located some 10 to 15 km to the north-northeast of the high reflectivity region at low levels. This was verified independently by Citation, ER-2 and radar observations.

It was evident from visual observations made from the Citation and from satellite imagery that the system was pulsating. Distinct regions of higher and more dense cloud could clearly be seen blowing

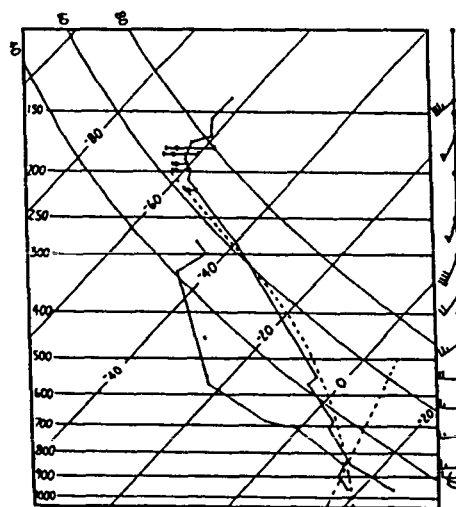


Fig. 1. 2100 GMT Chickasha (CHK) sounding. Wind barbs in knots. Horizontal bars with circles are ranges of Citation measurements within mean values at each level.



Fig. 2. South-north vertical cross section of Cimarron radar reflectivity data, corresponding to Citation pass #6.



Fig. 3. 35 mm photograph of overshooting tower D taken at 2112 GMT.

off downwind of the active storm region. The height of the anvil cloud top as measured by the ER-2 lidar varied from 10.5 to 11.5 km, and overshooting top heights reached 12.8 km. The 2100 GMT CHK sounding shows that a stable layer existed between 11.5 and 12.2 km and a nearly isothermal layer from 12.2 to 12.7 km capped by a strong inversion. A 35mm picture (Fig. 3) taken from the Citation shows the general appearance of cloud top.

The Citation made measurements in the vicinity of the storm between 2122 and 2315 GMT. During this two hour period six traverses along the length of the anvil were flown and active higher towers were penetrated ten times. All flight lines but the last (at 11.3 km) were flown at altitudes between 11.9 and 12.5 km MSL. All but one of the tower penetrations were made aligned approximately with the environmental winds. By graphically advecting the cloud top debris at  $24 \text{ ms}^{-1}$  toward the north-northeast and comparing the relative positions of the top penetrations in space and time, it was determined that six separate turrets were sampled. A list of the penetrations is given in Table 1.

The Citation was equipped to measure the state parameters, three-dimensional winds and cloud microphysics. Air motions were derived from 24 Hz data samples from a Litton LTN-76 Inertial Navigation System and a Rosemount 858AJ Flow Angle Sensor. The scheme of Lenschow (1972) was used to calculate the horizontal and vertical wind components. Cloud particle information was available from Particle Measuring Systems 2D

Table 1. Summary of tower penetrations

Pass #	Time (GMT)	Altitude (km)	Tower ID	Distance Incloud (km)	Aircraft Track (°)
1	212320	12.4	A	3.3	010
2	214531	12.4	B	1.3	155
3	215029	11.9	C	1.8	180
4	220005	12.5	C	0.1	190
5	220545	11.9	C	5.0	360
6	221328	11.9	D	3.6	190
7	221708	12.1	D	3.9	360
8	222003	12.1	D	4.8	090
9	231302	12.4	E	5.5	360
10	231302	11.3	F	7.8	185

cloud, 1D precipitation and FSSP probes. The FSSP data were used only as a qualitative indicator of the presence of ice crystals because the instrument response to frozen hydrometeors is unknown. The 2D data were processed using an artifact rejection scheme developed by Cooper (1978).

### 3. RESULTS

The results from the first three tower penetrations are shown in Fig. 4. The thermodynamic, dynamic and microphysical characteristics of the overshooting storm tops will now be presented.

#### 3.1 Equivalent Potential Temperature

The thermodynamic properties of the cloud tops and their immediate environment have been examined in terms of the equivalent potential temperature field ( $\theta_e$ ). Since most penetrations were made aligned with the anvil-level winds, perturbations from the mean flight line values represent profiles along these winds. The ranges and mean values of conditions sampled by the Citation are shown on the upper portion of the sounding in Fig. 1.

Several general characteristics are worth noting. In almost every case  $\theta_e$  is higher downwind of the tower than upwind, except within 1 km of the cloud boundary. On three of four passes made at 12.4 and 12.5 km, there was a strong positive perturbation of 3 K to 8 K near the upwind boundary (Fig. 4 a,b). On several passes there was a suggestion of a wave disturbance downwind of the towers as evidenced by alternating pockets of warmer and colder air (Fig. 4a). The wave length ranged from 5 to 10 km. In-cloud perturbations ranged from -4 K to +5 K at 12.4 km, but were less than 1.5 K at lower levels. For three of the four passes, higher  $\theta_e$  was found in cloud on the upwind side and lower  $\theta_e$  on the downwind side (as in Fig. 4a). The two towers which were sampled more than once showed warming with time.

The highest values of  $\theta_e$ , 351 K, were measured just out of cloud top at 12.5 km. This is approximately equal to the  $\theta_e$  at 12.8 km, the cloud top height sensed by the ER-2. The lowest values of  $\theta_e$  were roughly the same for each penetration altitude, indicative of air being brought up from lower levels. It is unclear as to why the average Citation temperatures are colder than the CHK sounding at these levels. During descent into Norman at 2330 GMT the Citation values were in close agreement with the 2300 CHK rawinsonde temperatures below 220 mb.

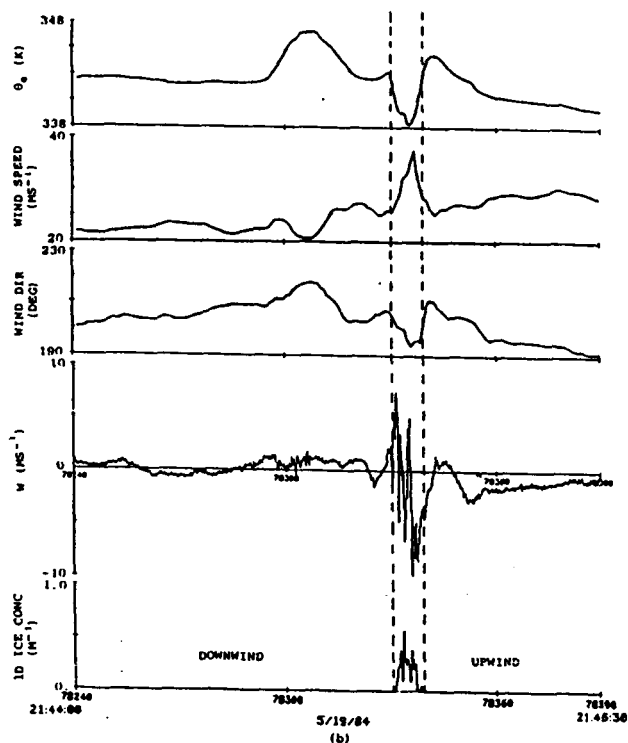
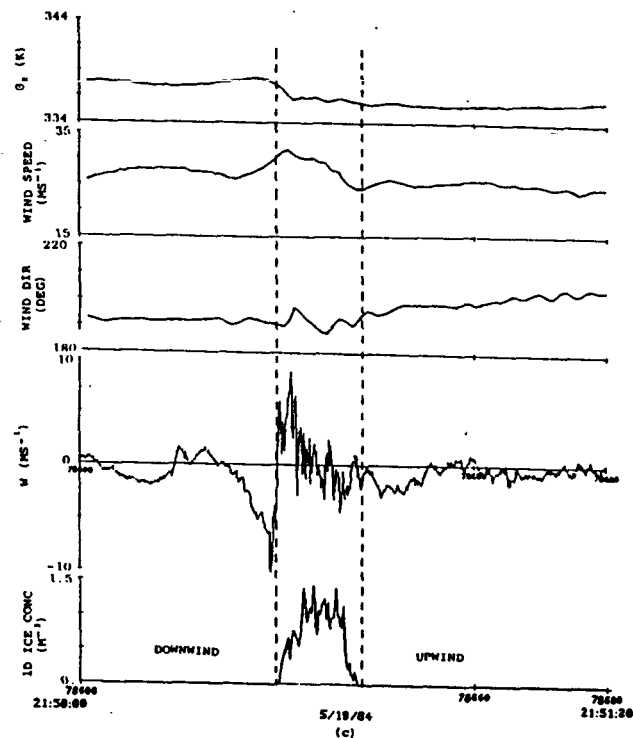
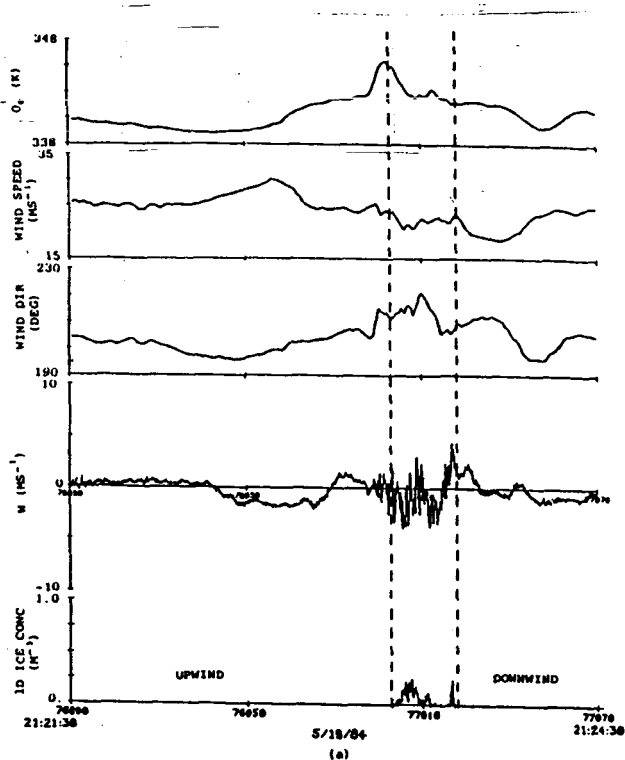


Fig. 4. Time series of equivalent potential temperature, horizontal wind speed and direction, vertical wind component, and 1D particle concentrations for passes (a) 1, (b) 2, and (c) 3. Vertical lines represent cloud boundaries.

### 3.2 Cloud Dynamics

The vertical wind ( $w$ ) and the horizontal wind field have been examined to investigate the dynamics of the overshooting tops and their interaction with the environment. The cloudy air in all towers contained relatively narrow (0.5 to 1.5 km diameter) regions of strong vertical velocities. Some tops contained several cores of upward and downward moving air as suggested by Newton (1966) and others (as in Fig. 4b). The largest positive values of  $w$  ( $5 \text{ ms}^{-1}$ ), excluding turbulent gusts, were found below 12 km while strong downward motions ( $-6 \text{ ms}^{-1}$ ) were encountered at all levels. The negative regions occurred at or near the cloud boundaries while positive motions were found primarily just to the upwind side of cloud center and near the downwind cloud boundary.

Outside of cloud the magnitude of  $w$  was generally less than or equal to  $2 \text{ ms}^{-1}$ . On most passes there were small regions of upward motion 1 to 2 km upwind and downwind of cloud boundaries. Otherwise no consistent patterns could be detected.

Horizontal wind speeds were compared to a mean environmental value of  $24 \text{ ms}^{-1}$  and perturbations were calculated. On a majority of the passes there was a reduction in speed from several kilometers upwind to cloud boundary (Fig. 4a,b). In cloud, speeds varied widely with both positive and negative fluctuations. However, in most cases (6 of 9), the speeds were higher in cloud than upwind (as in Fig. 4b,c). Up to 4 km downwind the perturbations were of the same sign as those in cloud. The wind direction showed a strong correlation with the temperature perturbations (Fig. 4b). The winds veered as the aircraft traversed from cold to warm regions.

## 5. CLOUD MICROPHYSICS

Although the microphysical properties of the towers were varied, a few general characterizations may be made. Nearly all towers had very distinct edges as defined by 2D-C counts. Particle concentrations dropped from an average of  $40\lambda^{-1}$  or more to zero in one second or less at the cloud boundaries. The clouds were composed entirely of ice crystals, primarily small ( $<200$  micron diameter) irregular particles. A sample of typical 2D images is given in Fig. 5. No liquid water was detected by a Rosemount icing rate meter, a Johnson-Williams probe or by visual observation of aircraft surfaces in flight. In addition to irregular particles, the 2D images showed some crystal aggregates and what appeared to be crystal branch fragments. There were also a few bullets and  $>1.0$  mm graupel particles.

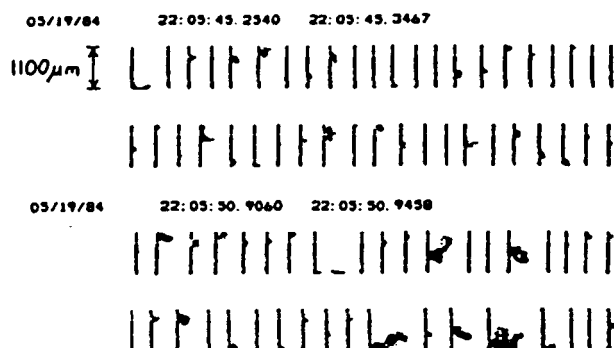


Fig. 5. 2D particle images from pass #5.

Concentrations measured by the 2D ranged from  $25\lambda^{-1}$  to  $200\lambda^{-1}$ . These estimates are probably low, however, because there were a large number of null images which were rejected by the processing software. These may have been the result of small ice crystals triggering the probe. The mean volume weighted diameter of the 2D particles ranged from 200 to 400 microns.

Peak concentrations of large particles (300-4500 micron diameter) varied from a few hundred to 500 per cubic meter. The 1D mean volume diameters ranged from 700 to 1200 microns. Higher concentrations of the larger particles were generally found in the upwind portion of the cloud with fewer near the cloud boundaries (Fig. 4a,c).

The two towers which were sampled more than once showed a decrease of particle size and concentrations with time. This decay was evident in both the 2D and the 1D data.

## 6. DISCUSSION

The cloud top region of a strongly sheared multicell cumulonimbus complex has been sampled in situ by an instrumented aircraft. A series of passes were made through the overshooting tops of the storm in order to investigate the nature of these tops and how they interact with their environment. The thermodynamic, dynamic and microphysical data gathered on this storm suggest several general characteristics of this cloud region. An attempt has been made to composite the measurements made on passes through six different

towers. The conclusions which follow are tentative because the measurements represent only snapshots of the towers at unknown points of their life cycles. Also, it is not known where the penetrations were made relative to the physical center of the towers.

The overshooting towers rose well above the mean top of the storm and penetrated the tropopause by several hundred meters before flattening against a strong inversion. This negatively buoyant air then mixed with the warmer environmental air and returned to a lower level but remaining above the tropopause. Large perturbations near cloud top indicate a downward mixing of lower stratospheric air in the vicinity of the tropopause. Mixing near cloud top and side boundaries may also be inferred from the lower concentrations and smaller sizes of ice particles found in those regions. The highest concentrations of large particles were found in the upwind portion of the cloud interior coincident with a general area of positive vertical motion.

There was strong subsidence measured near both the upwind and downwind boundaries. This may have been due either to the sinking of negatively buoyant air or to divergent flow at cloud top and mass continuity; there was no consistent correlation between vertical air motions and  $\Theta_e$  anomalies. A larger scale air flow may be inferred from the  $\Theta_e$  field. The occurrence of relatively lower  $\Theta_e$  values upwind and higher values downwind was likely the result of air with a lower  $\Theta_e$  rising on the upwind side and/or air with a high  $\Theta_e$  descending downwind.

The deceleration of the horizontal wind just upwind of the towers is suggestive of a stagnant point in flow around a solid object. Those passes where higher velocities were found in cloud and downwind may have been made near the side of the tower rather than through the center.

## ACKNOWLEDGEMENTS

This work was supported by NASA Grant NAG5-541.

## REFERENCES

- Adler, R.F., M.J. Markus, D.D. Fenn, G. Szejwach and W.E. Shenk, 1983: Thunderstorm top structure observed by aircraft overflights with an infrared radiometer. *J. Climate Appl. Meteor.*, 22, 579-593.
- Cooper, W.A., 1978: Cloud physics investigations by the University of Wyoming in HIPLEX 1977, Final Report. University of Wyoming, Laramie, 320 pp.
- Danielsen, E.F., 1982: A dehydration mechanism for the stratosphere. *Geophys. Res. Lett.*, 9, 605-608.
- Heymsfield, G.M., R.H. Blackmer, Jr. and S. Schotz, 1983: Upper-level structure of Oklahoma tornadic storms on 2 May, 1979. I: Radar and satellite observations. *J. Atmos. Sci.*, 40, 1740-1755.
- Lenchow, D.H., 1972: The measurement of air velocity and temperature using the NCAR Buffalo aircraft measuring system. NCAR Tech Note EDD-74.
- Newton, C.W., 1966: Circulations in large sheared cumulonimbus. *Tellus*, 18, 699-712.
- Roach, W.T., 1967: On the nature of the summit areas of severe storms in Oklahoma. *Quart. J. Roy. Meteor. Soc.*, 93, 318-336.
- Sauders, P.M., 1962: Penetrative convection in stably stratified fluids. *Tellus*, 14, 177-194.
- Shenk, W.E., 1974: Cloud top height variability of strong convective cells. *J. Appl. Meteor.*, 13, 917-922.